HHS Public Access

Author manuscript

Mater Res Lett. Author manuscript; available in PMC 2019 March 07.

Published in final edited form as:

Mater Res Lett. 2017 ; 5(8): 584–590. doi:10.1080/21663831.2017.1376720.

Microfluidics-mediated self-template synthesis of anisotropic hollow ellipsoidal mesoporous silica nanomaterials

Nanjing Hao, **Yuan Nie**, **Amogha Tadimety**, **Andrew B. Closson**, and **John X.J. Zhang***

Thayer School of Engineering, Dartmouth College, 14 Engineering Drive, Hanover, New Hampshire 03755, United States.

Abstract

Herein, a facile strategy was firstly developed to synthesize ellipsoidal mesoporous silica nanomaterials (MSNs) with well-ordered parallel channels along the short axis. A miniaturized microfluidic device with spiral-shaped channels was then chosen as a straightforward and general platform to produce the corresponding hollow counterparts of MSNs under mild conditions. Such reaction process carried out in a microfluidic system was further demonstrated to be more rapid and efficient than conventional batch method under equivalent experimental conditions. The evolution of hollow structure can be well-tuned by flow rates (*i.e.*, etching time), providing new paradigm for rational design and engineering of anisotropic nanostructures.

Keywords

Microfluidics; self-template; anisotropic; hollow; silica

1. Introduction

Mesoporous silica nanomaterials (MSNs) have attracted considerable attentions in various fields because of their many superior properties, such as relatively high surface area, large pore volume, good mechanical stability and biocompatibility [1]. Over the past two decades, great efforts have been devoted to the rational design of MSNs for maximizing their application efficacies through optimization of the physicochemical characteristics, including particle size, pore, and surface chemistry. However, a majority of reported materials are those of spherical shape, and research on anisotropic shaped MSNs still lags behind [2]. Recent evidences, from both experimental and theoretical aspects, reveals that the shapes of nanomaterials play significant roles on their performance [3–5]. Therefore, developing facile strategies to synthesize anisotropic shaped MSNs are in great challenge but also in great demand.

* john.zhang@dartmouth.edu.

Impact Statement: This study developed a straightforward and general microfluidic platform to produce hollow nanostructures, providing new routes for rational design and engineering of functional nanomaterials.

Disclosure statement

No potential conflict of interest was reported by the authors.

Hollow mesoporous silica nanomaterials (HMSNs) as one kind of MSNs with typical thin shell and large inner void have already shown unique advantages in sensing, drug delivery, energy, and catalysis fields [6]. The formation of HMSNs can be generally realized by either hard template strategy (such as TiO_2, Fe_3O_4, gold, and polystyrene nanoparticle as inner core) or soft template strategy (such as emulsion droplet, supramolecular micelle, and polymer vesicle as support material) [6,7]. However, both strategies have some inherent drawbacks. For example, in these cases, the template-removal process should undergo by either calcination at elevated high temperature or selective dissolution in strong acidic/basic solvents, which is often time-consuming and results in the resultant products with uncontrollable deformations. Therefore, there are still very limited methods for controllable synthesis of HMSNs, and even fewer for anisotropic shaped HMSNs [8,9].

Different from macroscale conventional batch reactor, microfluidic reactor as a newly developed technique offers an alternative promising platform for nanomaterials synthesis due to its special capabilities for delicate control on the microscale over diffusion and mixing in fluid flow [10,11]. In principle, microfluidic reactor allows precise flow rate measurement, intensive mixing, and rapid chemical reaction kinetics that conventional batch reactors can hardly reach [12]. Greatly reduced reactor dimensions are also beneficial for minimizing the local variations during the synthetic process. And most importantly, microfluidic reactor enables the reactions to be carried out in a stable and continuous way under automated conditions, which is essentially favorable for the reproducible synthesis of nanomaterials.

Herein, we firstly developed a facile strategy to synthesize ellipsoidal mesoporous silica nanomaterials (EMSNs) with well-ordered parallel channels along the short axis using cetyltrimethylammonium bromide (CTAB) and tyrosine as structure directing agents and tetraethyl orthosilicate (TEOS) as a silica precursor in dilute ammonia solution. Miniaturized microfluidic device with spiral-shaped channels was then chosen as a self-template directing tool to produce the hollow counterparts of EMSNs using phosphate buffered saline (PBS) as the etching agent and bovine serum albumin (BSA) protein as the surface protective coating agent at room temperature. The comparison of efficiency between microfluidic reactor and conventional batch reactor, the capability of such microfluidic reactor as a general platform for producing hollow MSNs, and the effect of flow rates (*i.e.*, etching time) on morphology changes were investigated. In addition, their potential applications in biomedicine were examined.

2. Methods

2.1 Synthesis of EMSNs

Briefly, CTAB (0.6 g) and tyrosine (0.3 g) were dissolved in 450 mL water, and then ammonia (25%, 4 mL) was added with gentle stirring for 20 min. TEOS (9 mL) was finally added dropwise with stirring, the mixture was centrifuged after 1 hour to collect the solid products. CTAB and tyrosine were removed with acidic ethanol (25 mL 37% HCl in 750 mL ethanol). After thoroughly washing and drying, the resultant white powder was yielded as EMSNs.

2.2 Fabrication of microfluidic device

The five-run spiral-shaped microchannel was fabricated from polydimethylsiloxane (PDMS) using soft lithography. Briefly, after designing the pattern with AutoCAD, film mask was obtained (from Fine Line Imaging, Inc.) to fabricate the master mold using standard photolithography. PDMS replica was then produced by pouring PDMS precursor onto the mold and curing the structures at 65 ºC for 3 hours. Microchannels were formed by bonding the PDMS replica to a standard glass slide after oxygen plasma treatment. The width and height of the microchannel are 500 μm and 50 μm, respectively. The smallest diameter of the spiral microchannel is 5.25 mm, and then it increases from 11.0 mm to 22.2 mm with an increment of 1.4 mm for each half run.

2.3 Synthesis of HEMSNs

To form hollow counterparts of EMSNs, EMSNs (90 mg) and BSA (9 mg) were dispersed in 30 mL water as one inlet flow and 30 mL PBS (pH 7.4, 2X) as the other inlet flow. The two inlet flows were pumped (PHD-2000, Harvard Apparatus) into the spiral microchannel both at a flow rate of 100 μL/min at room temperature and the as-synthesized products were collected at the outlet. As a comparison, all the above reactants were put into a 100 mL beaker as conventional batch reactor for chemical reactions under same conditions.

2.4 Drug loading, release, and in vitro cytotoxicity test

To load Doxorubicin (Dox), nanomaterials were mixed with Dox (2.8 mM) in a weight ratio of 1:1. The mixture was gently stirred at 37 °C under dark conditions, followed by centrifugation and washing twice with water to obtain EMSNs-Dox and HEMSNs-Dox. For the drug release, EMSNs-Dox and HEMSNs-Dox samples were immersed in PBS, and the supernatant was collected at given time intervals. The loading and release amount of Dox was determined by UV/vis spectroscopy at 233 nm using a standard calibration curve of Dox. Drug releasing results were obtained in triplicates. The cytotoxicity of EMSNs, HEMSNs, EMSNs-Dox, HEMSNs-Dox, and free Dox was evaluated using the CCK-8 viability assay. SK-BR-3 and HEK-293 cells were seeded at a density of 8000 cells per well in 96-well plates. After incubating cells with tested substrates for 24 h, 10 μL CCK-8 reagent was added to each well and incubated for 4 h. The absorbance of the resulting solution in each well was recorded at 450 nm with a microplate reader (TECAN SPARK 10M).

3. Results and discussion

Anisotropic ellipsoidal mesoporous silica nanomaterials (EMSNs) were synthesized using cetyltrimethylammonium bromide (CTAB) and tyrosine as structure directing agents, tetraethyl orthosilicate (TEOS) as silica precursor, and dilute aqueous ammonia as catalyst. As shown in Figure 1, well-defined EMSNs with an average long axis length of ~150 nm and an average short axis width of ~80 nm can be successfully obtained, and the mesoporous channels can be obviously seen as running parallel to the short axis (Figure 1E). Such well-ordered and relatively short channels promise great possibilities for mass transfer applications. Nitrogen sorption results showed that EMSNs exhibit a type IV isotherm (Figure S1A), typical for hexagonal cylindrical mesoporous channels [13]. The pore size of

EMSNs was measured to be 2.78 nm by the Barrett-Joyner-Halenda (BJH) method (Figure S1B). The pore volume and Brunauer-Emmett-Teller (BET) surface area were calculated to be 0.81 $cm^3\ g^{-1}$ and 923.7 $m^2\ g^{-1}$, respectively. Tyrosine plays a dominant role while others have relatively minor effects on the formation of EMSNs. Especially, only near-spherical mesoporous silica nanoparticles can be observed in the absence of tyrosine (Figure S2), indicating its important and essential role for assisting the growth of anisotropic ellipsoidal nanostructures.

To form the hollow counterparts of EMSNs, we chose a miniaturized microfluidic reactor with special spiral channel because of its superior properties for microreactions, such as low Reynolds number and transverse Dean flow across the channel [14], which will facilitate the efficient and intensive mixing and thus greatly shorten the reaction time compared to conventional batch reactors. As shown in Figure 2A, microfluidic device having five-run spiral microchannel was designed with two inlets for mixing the reactants and one outlet for collecting the resultant products. These two inlets for introduction of multiple starting reagents, the enhanced mixing properties of the spiral pattern, and the compact placement of microchannels with a relatively long length make this microreactor platform advantageous for carrying out chemical reactions. Specifically, EMSNs and BSA protein were dispersed in water as one inlet flow and equivalent volume of PBS (pH 7.4, 2X) as the other inlet flow. The two inlet flows were pumped into the spiral microchannel both at a flow rate of 100 μL/min at room temperature. Since the isoelectronic point of BSA protein is ~4.9 [15], it can be easily adsorbed onto the surface of EMSNs via the electrostatic attraction before they meet PBS to initiate the microreactions. The Reynolds number of such microreactor was calculated to be 135, indicating the presence of laminar flow inside microchannel. Comsol simulation result of mixing in microfluidic spiral channel further revealed its rapid and efficient capabilities for chemical reactions (Figure 2B).

As shown in Figure 3, well-defined HEMSNs with a typical thin shell layer of ~10 nm and large hollow void can be successfully obtained from the miniaturized microfluidic spiral-shaped reactor. HEMSNs retained the morphology of EMSNs without any apparent changes in the particle length and width, but the mesochannels of HEMSNs seem a little blurry and are not as ordered as that of EMSNs (Figure 3E), probably due to the etching action of PBS. After thermal decomposition to remove BSA protein (Figure S3), nitrogen sorption results of HEMSNs showed that, compared to EMSNs, the BJH pore size was increased to 3.03 nm, and the pore volume and BET surface area were changed to 0.45 $cm^3\ g^{-1}$ and 520.4 $m^2\ g^{-1}$, respectively (Figure S4). Using the same protocol, well-defined hollow spherical and rod-shaped mesoporous silica nanostructures can be also formed (Figures S5-6). In addition, microreactor enabling introduction of flows into the curved microchannels at a lower Reynolds number showed considerable improvement of mixing performance as compared to that of batch reactor. The transition time from EMSNs to HEMSNs via microreactor is less than 4 seconds (see calculation details in the Supporting Information), whereas, the batch reactor needs at least 18 hours to make EMSNs evolve into their hollow counterparts under same reaction conditions (Figure S7). These results reveal that such microfluidic spiral-shaped reactor can not only be acting as a general platform to produce hollow nanostructures but also exhibit more rapid and efficient capabilities than conventional batch reactors.

We further separately investigated the specific roles of PBS, BSA protein, and flow rates (*i.e.*, etching time) in the microfluidic reaction system. When the PBS was replaced with water, the nanostructures of EMSNs were still intact and no obvious etching effect can be observed (Figure S8). In the absence of BSA protein as a surface protective layer, both the surface and inner matrix of EMSNs were eroded and no intact nanostructures can be obtained (Figure S9). The effect of the flow rates on the morphology changes of EMSNs was also examined to understand etching time. As shown in Figure 4, the etching extent of EMSNs was gradually decreased with increasing flow rates. At 1000 μL/min (0.38 s etching time), the product from the outlet maintained almost complete structures of EMSNs, and only the mesoporous channels were slightly etched but still can be seen vaguely. When the flow rate was set as 500 μL/min (0.75 s etching time), the ordered mesoporous channels disappeared, but a majority of the inner matrix of EMSNs was still retained. Comparatively, at 200 μL/min (1.88 s etching time), the inner matrix of EMSNs began to be dissolved and hollow inside became to some extent appeared. At a flow rate of 100 μL/min (3.76 s etching time), well-defined hollow ellipsoidal nanostructures with a robust shell and large inner void were formed. However, when the flow rates continue to go lower, such as 50 μL/min (7.52 s etching time) and 20 μL/min (18.81 s etching time), even the shell of the hollow nanostructures can be partly etched and finally evolve into irregular pieces. These results not only help for revealing the morphology evolution process of hollow nanostructures but also help for fully understanding of the nano-bio interactions, especially stability and biodegradability [16].

Non-spherical micro-/nanomaterials have already shown great potentials in diverse applications [7,17,18]. Owing to their special anisotropic ellipsoidal shape, relative rich and short pore passages, and high pore volume, both EMSNs and HEMSNs will be also ideal for many applications, especially for those involving mass transfer. We then investigated their drug loading capacity toward Doxorubicin (Dox, an anticancer drug), drug release profile in different physiological pH conditions, and cancer cell inhibition activity against SK-BR-3 cells. The amounts of Dox loaded into EMSNs and HEMSNs were determined to be 358.9 and 467.4 mg per gram of nanomaterials, respectively, indicating the superior drug loading capacity of these anisotropic nanostructures compared to conventional shapes [19,20]. The drug release tests of Dox-loaded nanomaterials, EMSNs-Dox and HEMSNs-Dox, were conducted at both single pH conditions (Figure 5A) and a single-step change of pH conditions from pH 7.4 to pH 4.5 (Figure 5B). Although all of them can be continuously released, Dox from EMSNs-Dox and HEMSNs-Dox showed varying degrees of pH-dependent release. At pH 7.4, both EMSNs-Dox and HEMSNs-Dox exhibited very similar slow release profiles and only nearly 12% of the drug was released after 48 hours. The drug release rates were increased with decreasing pH (Figure S10). At even lower pH condition (pH 4.5), the drug release rates of EMSNs-Dox and HEMSNs-Dox can be increased to 65.4% and 76.1%, respectively. For the pH conditions with a single-step change of pH values, relatively slow release profile was observed in the first phase (pH 7.4) and then obviously rapid release happened in the second phase (pH 4.5). The differences in drug release rates, especially in acidic conditions, may be caused by the difference of their pore sizes. This kind of precisely pH-controllable drug release manner makes these anisotropic nanostructures an ideal nanomedicine platform for cancer therapy due to the pH difference

between acidic intracellular compartments of cancer cells and neutral extracellular space [21]. Cytocompatibility results showed that both EMSNs and HEMSNs exhibit no significant adverse effect on the cell viability of SK-BR-3 cells (up to 1000 μg mL^{-1}), but HEMSNs-treated cells have a relatively higher cell viability than EMSNs-treated ones (Figure 5C). These results were confirmed by the normal cell line HEK-293 (Figure S11). The cancer cell inhibition results further revealed that, compared to free Dox, both EMSNs-Dox and HEMSNs-Dox show stronger cell inhibition efficacy (Figure 5D). The half inhibitory concentration (IC_{50}) of free Dox is 2.6-fold of EMSNs-Dox and 3.6-fold of HEMSNs-Dox, respectively, which may be probably caused by the enhanced cellular uptake of the anisotropic shaped drug nanocarriers and the following effective targeted drug release inside cells. In addition, the relatively higher cancer cell inhibition rate of HEMSNs-Dox than that of EMSNs-Dox also agrees well with their in vitro drug release profiles (Figures 5A-B).

4. Conclusions

In summary, we firstly developed anisotropic EMSNs with well-ordered parallel channels along the short axis using CTAB and tyrosine as structure directing agents. A miniaturized spiral-shaped microfluidic device was then chosen as a self-template directing tool to successfully produce HEMSNs using PBS as the etching agent and BSA protein as the surface protective coating agent at room temperature. Such microfluidic reactor was demonstrated to be a general platform for producing hollow nanostructures and exhibited more rapid and efficient capabilities than conventional batch reactor. The shape evolution toward hollow nanostructure was primarily determined by the flow rates (*i.e.*, etching time). Both EMSNs and HEMSNs exhibited superior performance in nanomedicine, such as high drug loading capacity, controllable drug release, and enhanced cancer cell inhibition activity. These results not only provide new routes to synthesize anisotropic nanomaterials but also help for systematically understanding of nano-bio interactions.

Supplementary Material

Refer to Web version on PubMed Central for supplementary material.

Acknowledgments

Funding

This work was sponsored by the NIH Director’s Transformative Research Award (R01HL137157), and NSF grants (ECCS 1128677, 1309686, 1509369).

References

[1]. Tang FQ, Li LL, Chen D. Mesoporous silica nanoparticles: synthesis, biocompatibility and drug delivery. Adv Mater. 2012;24:1504–1534. [PubMed: 22378538]

[2]. Hao NJ, Li LF, Tang FQ. Roles of particle size, shape and surface chemistry of mesoporous silica nanomaterials on biological systems. Int Mater Rev. 2017;62:57–77.

[3]. Yang K, Ma YQ. Computer simulation of the translocation of nanoparticles with different shapes across a lipid bilayer. Nat Nanotechnol. 2010;5:579–583. [PubMed: 20657599]

[4]. Hao NJ, Li LF, Tang FQ. Shape matters when engineering mesoporous silica-based nanomedicines. Biomater Sci. 2016;4:575–591. [PubMed: 26818852]

[5]. Geng Y, Dalhaimer P, Cai SS, et al. Shape effects of filaments versus spherical particles in flow and drug delivery. Nat Nanotechnol. 2007;2:249–255. [PubMed: 18654271]

[6]. Lou XW, Archer LA, Yang ZC. Hollow micro-/nanostructures: synthesis and applications. Adv Mater. 2008;20:3987–4019.

[7]. Hao NJ, Li LF, Tang FQ. Facile and tunable synthesis of hierarchical mesoporous silica materials ranging from flower structure with wrinkled edges to hollow structure with coarse surface. J. Nanopart. Res. 2016;18:321.

[8]. Hao NJ, Li LF, Tang FQ. Facile preparation of ellipsoid-like MCM-41 with parallel channels along the short axis for drug delivery and assembly of Ag nanoparticles for catalysis. J Mater Chem A. 2014;2:11565–11568.

[9]. Hao NJ, Chen X, Jeon S, et al. Carbohydrate-conjugated hollow oblate mesoporous silica nanoparticles as nanoantibiotics to target mycobacteria. Adv Healthc Mater. 2015;4:2797–2801. [PubMed: 26450697]

[10]. Elvira KS, Solvas X, Wootton RCR, et al. The past, present and potential for microfluidic reactor technology in chemical synthesis. Nat Chem. 2013;5:905–915. [PubMed: 24153367]

[11]. Marre S, Jensen KF. Synthesis of micro and nanostructures in microfluidic systems. Chem Soc Rev. 2010;39:1183–1202. [PubMed: 20179831]

[12]. Park J, Saffari A, Kumar S, et al. Microfluidic synthesis of polymer and inorganic particulate materials. Annu Rev Mater Res. 2010;40:415–443.

[13]. Sing KSW, Everett DH, Haul RAW, et al. Reporting physisorption data for gas/solid systems with special reference to the determination of surface area and porosity. Pure Appl Chem. 1985;57:603–619.

[14]. Sudarsan AP, Ugaz VM. Fluid mixing in planar spiral microchannels. Lab Chip. 2006;6:74–82. [PubMed: 16372072]

[15]. Hudson S, Cooney J, Magner E Proteins in mesoporous silicates. Angew Chem Int Ed. 2008;47:8582–8594.

[16]. Hao NJ, Liu HY, Li LL, et al. In vitro degradation behavior of silica nanoparticles under physiological conditions. J Nanosci Nanotechnol. 2012;12:6346–6354. [PubMed: 22962747]

[17]. Champion J, Katare YK, Mitragotri S Particle shape: a new design parameter for micro- and nanoscale drug delivery carriers. J Control Release. 2007;121:3–9. [PubMed: 17544538]

[18]. Hao NJ, Chorsi HT, Zhang XJ. Hierarchical Lotus Leaf-Like Mesoporous Silica Material with Unique Bilayer and Hollow Sandwich-Like Folds: Synthesis, Mechanism, and Applications. ACS Sustain Chem Eng. 2017;5:2044–2049.

[19]. Hao NJ, Jayawardana KW, Chen X, et al. One-step synthesis of amine-functionalized hollow mesoporous silica nanoparticles as efficient antibacterial and anticancer materials. ACS Appl Mater Interfaces. 2015;7:1040–1045. [PubMed: 25562524]

[20]. Gu J, Su S, Zhu M, et al. Targeted doxorubicin delivery to liver cancer cells by PEGylated mesoporous silica nanoparticles with a pH-dependent release profile. Microporous Mesoporous Mater. 2012;161:160–167.

[21]. Warburg O On the origin of cancer cells. Science. 1956;123:309–314. [PubMed: 13298683]

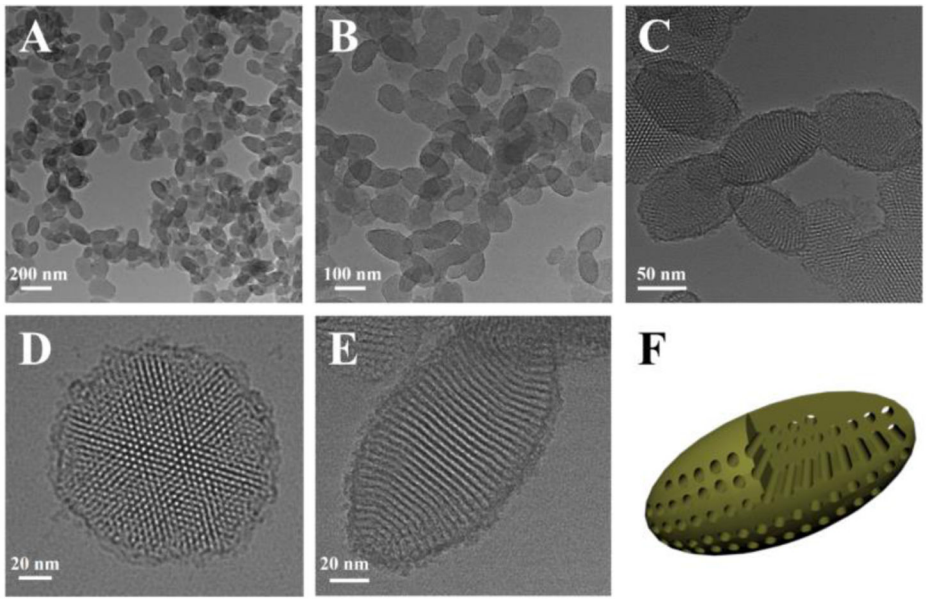

Figure 1.
(A-C) TEM images of EMSNs at different magnifications. (D) and (E) are the top-view and side-view images of single EMSN, respectively. (F) A schematic illustration of the ellipsoidal nanoparticle with parallel mesoporous channels along the short axis.

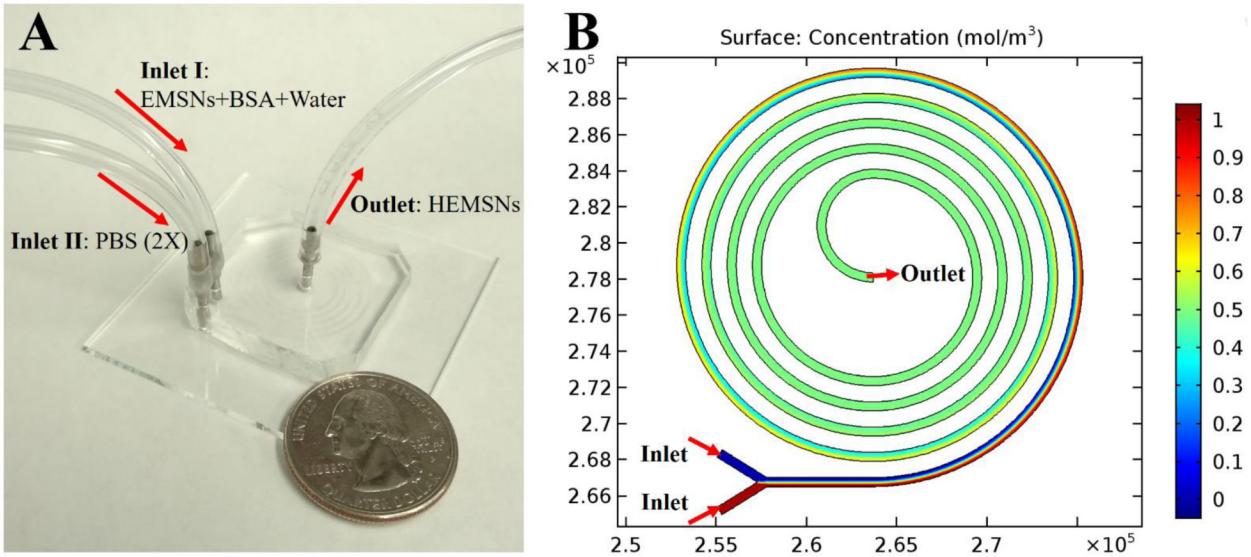

Figure 2.

(A) Experimental set up for the microfluidic synthesis of HEMSNs, with a quarter-dollar coin for scale. (B) Comsol simulation result of mixing in microfluidic spiral channel, where two flows having different concentrations could achieve complete mixing within about one run (see simulation details in SI).

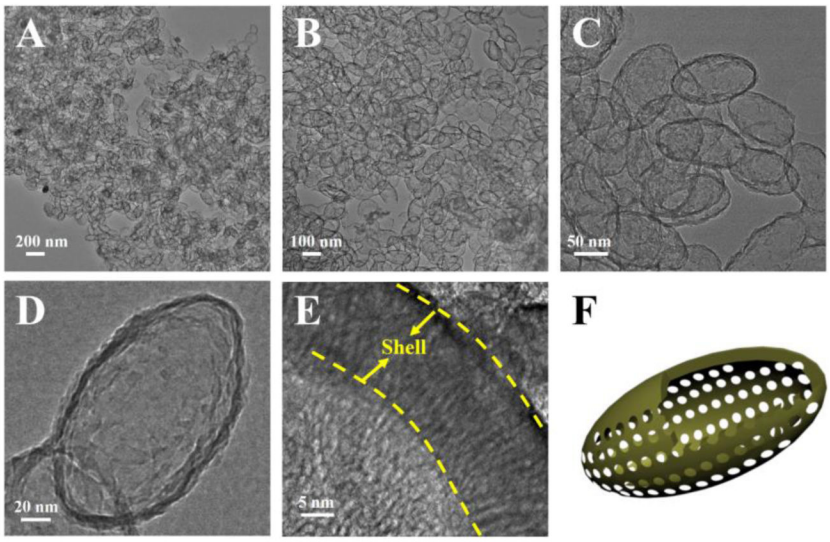

Figure 3.
(A-E) TEM images of HEMSNs at different magnifications. (F) A schematic illustration of the hollow ellipsoidal nanoparticle with typical shell and inner void.

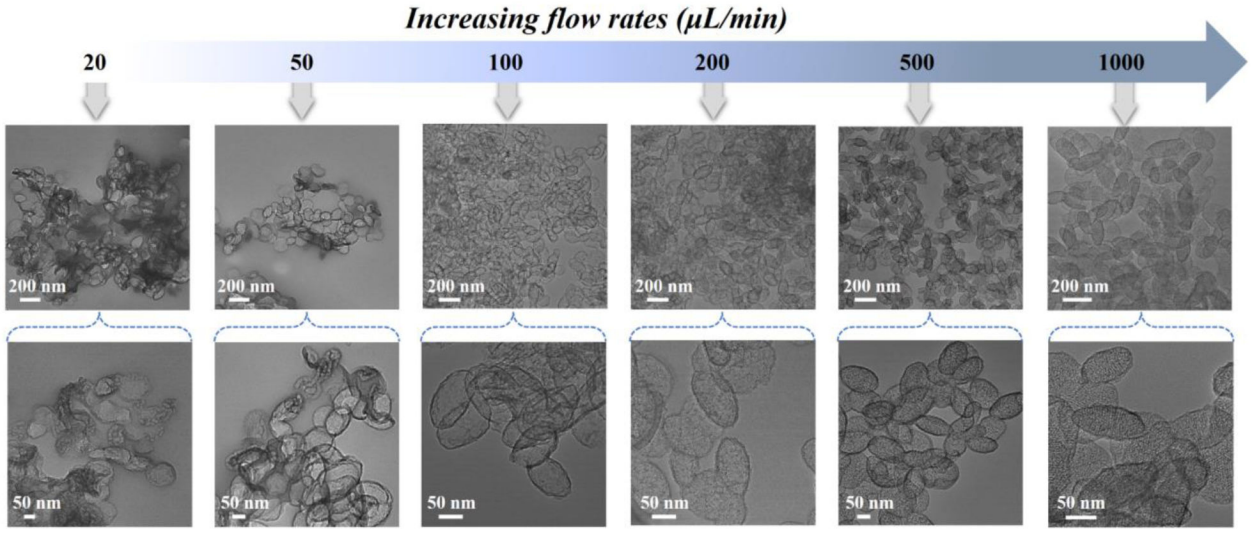

Figure 4.
The effect of the flow rates (*i.e.*, etching time) on the morphology changes of EMSNs.

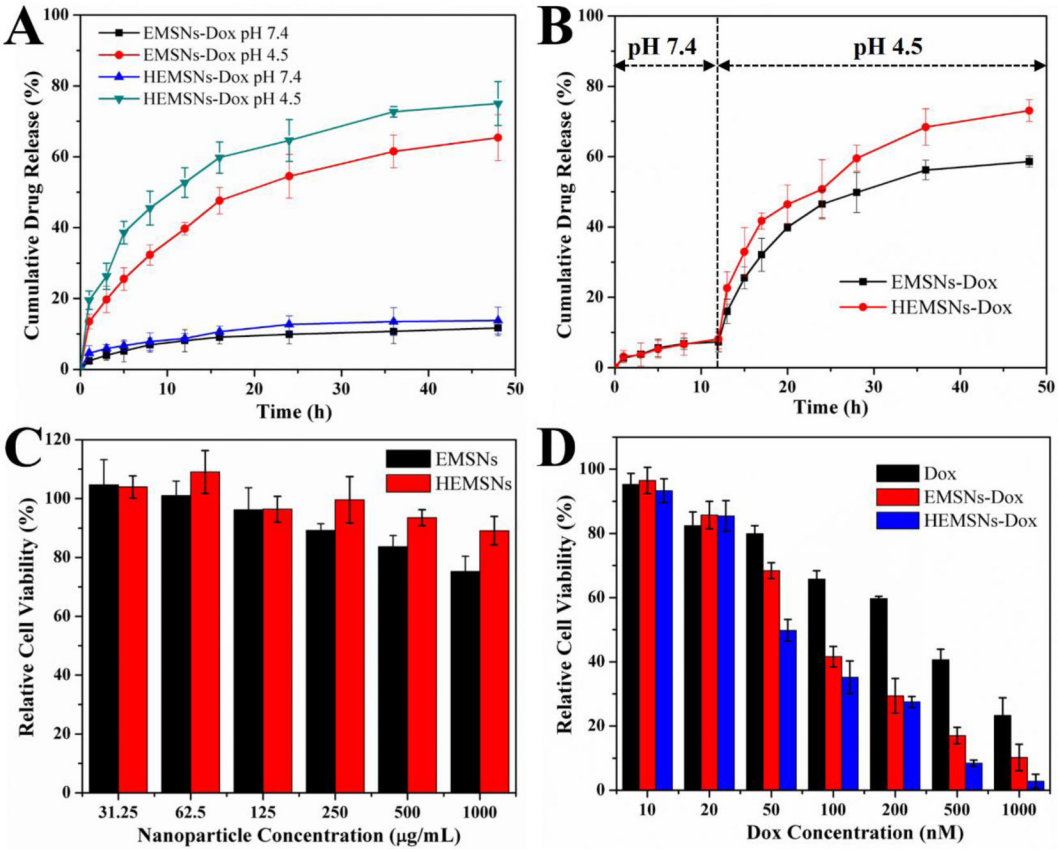

Figure 5.

Comparison of drug release profiles and in vitro cytotoxicity tests. (A-B) Release profiles of Dox from EMSNs-Dox and HEMSNs-Dox in both single pH 4.5 and pH 7.4 conditions (A), and a single-step change in the pH condition from pH 7.4 to pH 4.5 (B). (C) SK-BR-3 cell viability with particle concentrations of EMSNs and HEMSNs from 31.25 to 1000 μg mL^{-1} for 24 h. (E) SK-BR-3 cell viability with Dox concentrations of free Dox, EMSNs-Dox, and HEMSNs-Dox from 10 to 1000 nM for 24 h.